README File

TROPOMAER (Version 1.1.1)

Released Date: October 20, 2021

1. Overview

The Tropospheric Monitoring Instrument (TROPOMI), onboard the Sentinel-5 Precursor (S5P) satellite, was launched on 13 October 2017. The TROPOMI mission is a follow-on to the successful AURA Ozone Monitoring Instrument (OMI) mission launched in late 2004 and still operational to date. TROPOMI is a high-spectral-resolution spectrometer covering eight spectral windows from the ultraviolet (UV) to the shortwave infrared (SWIR) regions of the electromagnetic spectrum. The instrument operates in a push-broom configuration, with a swath width of about 2600 km on the Earth's surface. The typical pixel size (near nadir) is 5.5x3.5 km^2 for all spectral bands, with the exception of the UV1 (5.5x28 km^2) and SWIR (5.5X7 km^2).

All S5P TROPOMI L1b data and L2 files for trace gas products, UV aerosol index and Oxygen-A band aerosol layer height, are currently generated by the Copernicus Sentinel project, and are made available by ESA for distribution in the USA through NASA GES DISC (GES DISC Data Release: Copernicus Sentinel-5P/TROPOMI Products Release News (nasa.gov)). The TROPOMI L2 388 nm aerosol optical depth (AOD) and single scattering albedo (SSA) L2 product is developed at NASA and distributed through NASA GES DISC. This document provides a description of the NASA Level-2 aerosol data products derived from S5P TRPOMI observations.

The NASA TROPOMI aerosol inversion procedure (TROPOMAER, Torres et al., 2020) is a direct application of the OMI near UV aerosol algorithm (OMAERUV, Torres et al., 2007; 2013). A brief explanation of TROPOMAER along with a detailed description of the TROPOMAER generated level 2 files are presented in this README document. For detailed information TROPOMAER scientific basis and on the inversion process itself readers are referred to Torres et al (2020) and other available publications on the heritage algorithm (Torres et al., 2007; 2013).

As in OMAERUV, the TROPOMAER algorithm uses top of the atmosphere (TOA) radiance measurements at 354 nm and 388 nm. The choice of wavelengths ensures continuity of the long-term record started with the OMI heritage product. Retrieved parameters for cloud-free conditions are 388 nm aerosol extinction optical depth (AOD) and single scattering albedo (SSA). For overcast conditions, TROPOMAER retrieves aerosol optical depth of aerosol layers above water clouds (ACAOD) along with the cloud optical depth (COD) of the underlying cloud layer (Torres et al., 2012; Jethva et al., 2018). All these parameters are retrieved at 388 nm but are also reported at 354 nm and 500 nm. In addition to the above physical parameters, TROPOMAER calculates a residual parameter that quantifies the difference in 354 nm to 388 nm spectral contrast between measured and calculated radiances assuming a purely molecular atmosphere. Because most

of the observed large positive residuals are associated with the presence of absorbing aerosols, this parameter is commonly known as the UV aerosol index (UVAI).

The information in this README file applies only to the first public release of the TROPOMAER data of collection 01. As subsequent data versions are produced and released, the README file will be updated accordingly to reflect the latest algorithm modifications and data quality assessments.

2. TROPOMAER UV Algorithm Description

2.1 Retrieval approach

TROPOMAER ingests TROPOMI level1b (L1b) radiance and irradiance data along with associated viewing geometry and other relevant ancillary information. In the global mode each L1B file contains a single orbit of data covering the sunlit portion of the Earth from pole-to-pole with a swath width of approximately 2600 km on the Earth's surface. Radiance and irradiance measurements at 354 and 388 nm in the UVIS detector from L1b BAND3 product (version 01) are fed to the aerosol algorithm.

As in the heritage algorithm, TROPOMAER uses a set of aerosol models to account for the presence of carbonaceous aerosols from biomass burning (BIO), desert dust (DST), and sulfate-based (SLF) urban/industrial aerosols (see Appendix 1). The optical depth and single scattering albedo values at 388 nm are inverted from TROPOMI TOA measurements of 354 and 388 nm radiances. Conversions to 354 and 500 nm are carried out to facilitate comparisons with measurements from other space-borne and ground based sensors, as well as with model calculations, which often report values at 500 nm. Because this transformation relies on the spectral dependence of the aerosol models assumed in the algorithm, the reported values at the other wavelengths, particularly those at 500 nm, should be considered less reliable.

For environments where cloud free conditions prevail, AOD can be reliably retrieved. Cloud interference with the satellite retrieval is minimal over arid and semi-arid regions where dust aerosols are commonly present. Clear skies are also frequent in areas of seasonal biomass burning and forest fires in the vicinity of the sources. As the plumes of dust and smoke aerosols drift away from their source regions, they mix with clouds and the AOD retrieval becomes very challenging.

The 388 nm ACAOD is retrieved along with the COD of the underlying water cloud [Torres et al., 2012; Jethva et al., 2018]. The ACAOD/COD retrievals are carried out over scenes of lofted layers of carbonaceous or dust particles above low-level cloud decks. While the spectral aerosol SSA assumed in the inversion is taken from the existing OMI-based daily regional climatology derived using cloud-free SSA retrievals [Jethva et al., 2018], the assumption of aerosol layer height relies on a 30-month long monthly global OMI-CALIOP combined dataset [Torres et al., 2013]. Like its cloud-free counterpart, the above-cloud AOD and COD are retrieved at 388 nm, and also reported at 354 nm and 500

nm based on the assumed wavelength dependence of extinction. Each valid retrieval of ACAOD and COD is assigned with an appropriate quality flag.

TROPOMAER retrieval results are reported in orbital level-2 (L2) files. In addition to the geo-location information associated with the geographic center of each TROPOMI pixel in the global observation mode as well as the geographical coordinates of the corners of each pixel. Ancillary information used in the inversion procedure is also included in the file. A detailed description of the product is given in section 4.

2.2 Ancillary Information

2.1.1 Surface Albedo

A global climatological data set of Lambertian surface reflectivity (R_{SFC}) *at 354 and 388 nm is used in TROPOMAER*. It was obtained using a multi-year record of scene reflectivity (R_{SCE}) obtained from OMI observations.

Over land, R_{SFC} is estimated as the minimum OMI observed R_{SCE} over 10-years (2005-2014) for every month of the year averaged over a 0.25°x0.25° geographical grid. This climatological data set differs from that of *Kleipool et al* [2008], used in OMI's trace gas retrieval algorithm, in that the resulting surface albedo is associated with the actual observed minimum value per grid per month and, therefore, more suitable for aerosol retrieval applications.

The ocean surface reflectivity is estimated in a similar way as over land with the addition of a correction for the Sun's specular reflection. The satellite derived R_{SCE} under cloud-free conditions over the ocean is approximated as the sum of two terms: a Lambert-equivalent Fresnel reflectivity (R_F) term and a second reflectivity term associated with water-leaving reflectance (R_W). The R_F term is obtained by calculating the upwelling radiance at the top of the atmosphere using an atmosphere-ocean radiative transfer model [*Cox and Munk*, 1954] for a chlorophyll-free ocean. The calculated radiance is then converted to a Lambert-equivalent reflectivity (LER) as defined by Chandrasekhar (1960), in which the calculated radiance is used in lieu of the observed one. The resulting R_F term varies with satellite viewing geometry. R_W is estimated empirically by subtracting R_F from R_{SCE}. The resulting minimum R_W values per grid per month are assumed here to represent the ocean R_{SFC}. The OMI-based surface reflectivity climatology is available from the PI upon request.

2.1.2 Aerosol Layer Height

The height above the surface of absorbing aerosol layers (desert dust and smoke particles) is given by a climatological data set derived from CALIOP observations [*Torres et al.,* 2013]. Although the climatology covers most regions of the globe where seasonally varying atmospheric loads of desert dust and carbonaceous aerosols are known to reside, there are cases where the CALIOP data base does not provide height information. In those instances, the height of DST aerosol layers is taken from a GOCART-generated climatology [*Ginoux et al.,* 2001]. A detailed description of aerosol layer height determination is given in section 2.2.2.

2.1.3 Real Time AIRS Carbon Monoxide (CO)

Since CO is the main gaseous component of biomass burning, it constitutes a reliable tracer of carbonaceous aerosol. The AIRS/Aqua L3 Daily Standard Physical Retrieval V006 CO product (AIRS3STD) is used in the aerosol algorithm to aid in the identification of carbonaceous aerosols. As used in TROPOMAER, AIRS3STD CO total column in molecules-cm^{-2} is reduced to a unitless index (COI), by dividing the AIRS reported CO measurement by 10^{18} molecules-cm^{-2} [*Torres et al.,* 2013].

2.2 TROPOMAER Aerosol Products

2.2.1 Absorbing UV Aerosol Index and Cloud Fraction

The UVAI is a measure of the departure of the spectral dependence of the near-UV upwelling radiation at the top of the actual Earth surface-atmosphere system from that of a hypothetical pure molecular atmosphere bounded at the bottom by a wavelength independent Lambertian surface. The UVAI calculated as shown in Eq. 1, was developed empirically from TOMS observations. In Eq. 3, λ_0 is the reference wavelength (388 nm) whereas λ is the wavelength at which AI is calculated (354 nm). Near-zero values of UVAI result when the radiative transfer processes accounted for in the simple Rayleigh scattering model adequately explain the observations. For a well-calibrated sensor, the non-zero residues are produced solely by geophysical effects, of which absorbing aerosols are by far the most important source of positive UVAI values. Non-absorbing aerosols yield small negative UVAI values but the difficulty to separate the non-absorbing aerosol signal from other non-aerosol related effects limits its usefulness.

$$UVAI = -100\left\{\log\left[\frac{I_{\lambda}^{obs}}{I_{\lambda_0}^{obs}}\right] - \log\left[\frac{I_{\lambda}^{cal}}{I_{\lambda_0}^{cal}}\right]\right\} = -100\log\left[\frac{I_{\lambda}^{obs}}{I_{\lambda}^{cal}}\right] \qquad (1)$$

The new method explicitly accounts for scattering effects of water clouds as described in detail by *Torres et al., 2018*. It is based on analytical studies showing that the use of Mie scattering theory reproduces remarkably well the satellite observed field of backscattered UV radiation in a cloudy atmosphere [*Ahmad et al.,* 2004]. In this approach, it is assumed that the radiance measured by the sensor at pixel level emanates from a combination of clear and cloudy conditions (I_{λ}^{s} and I_{λ}^{C}) involving a cloud of fixed optical depth and varying cloud fraction. The I_{λ}^{s} term is calculated from the Lambertian approximation formulation (Chandrasekhar, 1960), using as input the wavelength dependent climatological values of surface albedo (derived from analysis of the 10-year long-term OMI record of minimum reflectivity) and a pure molecular atmospheric model for surface pressured adjusted for topography. The I_{λ}^{C} terms, on the other hand, are calculated using Mie scattering theory for an assumed water cloud model [*Deirmendjian,* 1964] and wavelength-dependent refractive index [*Hale and Querry*, 1973], at prescribed top and

bottom levels (700 and 800 hPa), and fixed cloud optical depth (COD). The choice of COD value of 10 is based on the highest frequency of occurrence of this value reported by MODIS observations [*King et al.,* 2013]. A wavelength independent radiative cloud fraction, f_C, is calculated from equation

$$f_C = \frac{I^{obs}_{\lambda_0} - I^{s}_{\lambda_0}}{I^{C}_{\lambda_0} - I^{s}_{\lambda_0}} \quad (2)$$

When the resulting cloud fraction is larger than unity, overcast sky conditions are assumed (i.e., f_C=*1.0*), and a new I^{C}_{λ} term for COD value larger than 10 that matches $I^{obs}_{\lambda_0}$ is derived. I^{cal}_{λ} values are then obtained by linearly combining the clear and cloudy sky contributions:

$$I^{cal}_{\lambda} = (1.0 - f_C) I^{s}_{\lambda} + f_C I^{C}_{\lambda} \quad (3)$$

The original LER approach will still be used in TROPOMAER under conditions of snow/ice presence at the surface as indicated by the surface quality flag available in the level 2 files. The LER approximation is also applied for high terrain regions with surface pressure lower than 600 hPa.

2.2.2 Aerosol Optical Depth and Single Scattering Albedo

In the UV, the reflectance of all terrestrial surfaces is very low compared to the atmospheric signal, therefore, the retrieval of aerosol optical depth is possible over both water and land surfaces, including the arid and semi-arid regions of the world that appear very bright in the visible and near-IR. In addition, the interaction between aerosol absorption and molecular scattering from below the aerosol layer allows the retrieval of aerosol single scattering albedo.

The current characterization of ocean reflective properties in the TROPOMAER algorithm does not explicitly account for ocean color effects and, therefore, the quality of the retrieved aerosol properties over the oceans for low aerosol amounts would be highly uncertain. For that reason, retrievals over the oceans are only carried out for high concentrations of either desert dust or carbonaceous aerosols as indicated by UVAI values larger than or equal to 1.0. Over the oceans UVAI values less than 1.0 are assumed to be associated with ocean color effects and/or low concentration weakly absorbing (or non-absorbing) aerosols.

- *Aerosol Models*

The TROPOMAER retrieval algorithm assumes that the column atmospheric aerosol load can be represented by one of three types of aerosols: desert dust (DST), carbonaceous aerosols associated with biomass burning (CRB), and sulfate-based aerosols (SLF). Each aerosol type is represented by seven aerosol models of varying single scattering albedo, for a total of twenty-one models. The micro-physical properties of the twenty-one aerosol

models used by TROPOMAER are based on long-term statistics of ground-based observations by the Aerosol Robotic Network (AERONET). The CRB and SLF aerosol types are modelled as poly-dispersions of spherical particles, whereas the DST models are treated now modelled as spheroids [Torres et al., 2018; Gassó and Torres, 2016]. For a full description of the aerosol models see Appendix 1. Radiance look-up tables at 354 and 388 nm with nodal points on viewing geometry, AOD, SSA and aerosol layer height are created using Mie Theory for spherical particles and T-matrix and Geometric Optics for spheroids [Dubovik et al., 2006].

- *Aerosol type selection*

Aerosol type determination is carried out on the basis of the magnitudes of the UVAI and COI parameters as illustrated in Fig. 1. Because of the lack of AIRS daily coverage, it is not always possible to use same-day COI values to infer aerosol type. Depending on AIRS data availability, COI may be determined based on current-day observations, previous day observations, or a monthly climatology. The actual source of COI data is documented in the *AIRSCO_Flags* data field with values from 1 to 3 as shown in Table 1.

Value of *AIRSCO_Flags* data field	**Source of COI data**
1	Current day
2	Previous day
3	Monthly Climatology

Table 1. COI determination

Threshold values of UVAI ($UVAI_0$) are 0.8 over land, and 1.0 over the oceans. COI threshold values (COI_0) are 2.0 and 1.6 for the northern and southern hemisphere respectively. COI_0 values are intended to remove background upper tropospheric CO which may not be necessarily associated with carbonaceous aerosols. A smoothing function in COI_0 is used to transition from SH to NH threshold values.

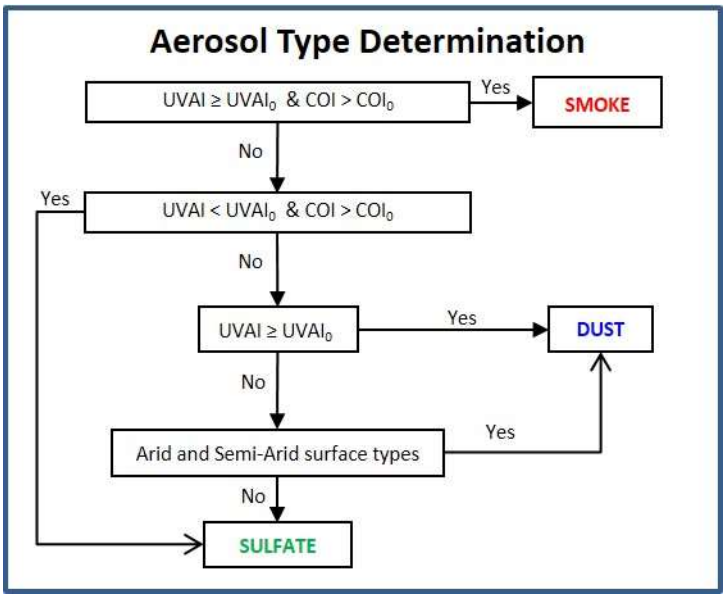

Figure 1. Flow diagram illustrating the aerosol type selection scheme.

-Cloud Screening

Sub-pixel cloud contamination is the largest source of uncertainty in satellite retrieved aerosol products. Algorithm quality flags 0 and 1 assign a level of confidence to the retrieved parameters. Flag 0 (highest confidence) is assigned to retrieval conditions when minimum cloud contamination is detected as determined by the adopted cloud mask, whereas Flag 1 is reported for conditions where cloud contamination is suspected. Although, the data is still reported for flag 1 retrievals, its quantitative use is not recommended. Because cloud contamination affects AOD and single scattering co-albedo (1-SSA) in opposite directions, a partial cancellation of errors may take place in the calculation of AAOD.

Alternatively, the VIIRS cloud mask information is also available in Level 2 file for replacing the existing cloud screening scheme (i.e., flag 0) with the value (=1.0) of "VIIRS_confidently_clear" field. A more detailed description of the S5p-NPP cloud product is available from the link (Sentinel-5 precursor/TROPOMI Level 2 Product User Manual NPP Cloud (copernicus.eu)). Since launch until early March 2020, TROPOMAER used an ESA-produced cloud mask based on sub-kilometer resolution radiance measurements at 1.385 μm by the NOAA (National Oceanic and Atmospheric Administration) Visible Infrared Imaging Radiometer Suite (VIIRS) on the S-NPP (Suomi-National Polar-orbiting Partnership) platform, re-gridded to the TROPOMI spatial resolution [Siddans, 2016]. On 7 March 2020 (TROPOMI orbit 12432), the initial NOAA VIIRS cloud mask used with TROPOMI was replaced with the NOAA Enterprise Cloud Mask (ECM) product.

- *Aerosol layer height*

The assumed aerosol level height is extracted from the CALIOP height climatology for each pixel as discussed in section 3.1.2. Although the CALIOP climatology provides information on aerosol layer height for most of the globe, there may be instances when no data is available. In those cases, the choice of aerosol layer height for absorbing aerosol layers varies with aerosol type and location.

Carbonaceous aerosol layers within 30 degrees of the Equator are assumed to have maximum concentration at 3 km above ground level, whereas smoke layers at mid and high-latitude (poleward of ±45˚) are assumed to peak at 6 km. The height of smoke layers between 30˚ and 45˚ latitude in both hemispheres is interpolated between 3 and 6 km with latitude.

The height of desert dust aerosol layers varies between 1.5 and 10 km and is taken from a multi-year climatological average of Chemical Model Transport (CTM) calculations using the GOCART model.

For the sulfate-based aerosols, the algorithm considers that the aerosol concentration is largest at the surface and decreases exponentially with height.

The *HeightFlags* data field provides information on the source of aerosol layer height used in the AOD/SSA retrieval. Value of *HeightFlags* varies from 1 to 4 as shown in Table 2.

Value of *HeightFlags* data field	**Source of aerosol layer Height information**
1	CALIOP Climatology
2	GOCART Climatology
3	Interpolated with latitude between 3 and 6 km
4	Assumed value (0.0, 1.5, 3.0, 6.0, or 10.0)

Table 2. Aerosol layer height determination

2.2.3 Retrieval Products

A summary of the retrieval criteria and retrieved parameters is presented in Table 3. As stated, retrievals take place over land for all cloud-free conditions. In addition of cloud-free conditions, the UVAI must be greater than unity for ocean retrievals.

Retrieved values of AOD, AAOD and SSA are reported at 388 nm. Similar values are also reported at 354 and 500 nm by conversion from the 388 nm retrieval. The wavelength conversion from 388 nm to 354 and 500 nm is done using the spectral dependence associated with the assumed aerosol particle size distribution and retrieved absorption information. The wavelength transformation for carbonaceous aerosols has been revisited to account for the presence of organic carbon.

Surface Category	*UVAI*	COI	Surface Type	Aerosol Type	Retrieved Parameters
Ocean	≥ 1.0	>2.0 NH (1.6 SH)	n/a	CRB	AOD, SSA
Ocean	≥ 1.0	≤2.0 NH (1.6 SH)	n/a	DST	AOD, SSA
Ocean	<1.0	-	-	-	No retrieval
Land	≥ 0.8	>2.0 NH (1.6 SH)	All	CRB	AOD, SSA
Land	≥ 0.8	≤ 2.0 NH (1.6 SH)	All	DST	AOD, SSA
Land	< 0.8	>2.0 NH (1.6 SH)	All	SLF	AOD, SSA
Land	< 0.8	≤ 2.0 NH (1.6 SH)	All but	SLF	AOD, SSA
Land	< 0.8	≤ 2.0 NH (1.6 SH)	arid	DST	AOD, SSA
			arid		

Table 3. Retrieval Approach Criteria

2.2.4 Algorithm Flag

A simplified algorithm flag scheme has been implemented. Flag categories and their description are summarized in Table 4.

Flag	Description
0	Minimum sub-pixel cloud contamination. Most reliable retrievals (AOD,
1	SSA, AAOD)
2	Possible Cloud contaminated retrievals, retrievals still reported.
3	No longer used.
4	Out-of-bounds SSA or AOD above 6.0 at 500nm.
5	Snow/ice contaminated data.
6	Solar Zenith Angle above threshold (70 degree).
7	Sun glint angle below threshold over water (40 degree).
	Terrain Pressure below threshold (250.0 hPa).

Table 4. Algorithm flag scheme

Flags 0 and 1 qualify the reliability of reported retrieved parameters in terms of sub-pixel cloud contamination effects. Flag 1 is reported for conditions where cloud contamination was suspected to be present. Although, the data is still reported for flag 1 retrievals, its quantitative use is not recommended.

Flags 3 through 7 document the occurrence of observational, geographical or environmental conditions preventing the retrieval of aerosol parameters and fill values for the retrieved parameters are reported in the respective pixel.

More detailed description of the algorithm is available in Torres et al., 2020 (https://doi.org/10.5194/amt-13-6789-2020).

3. Data Quality Assessment

Because of the relatively large footprint of the TROPOMI observations (5.5x3.5 km^2 at nadir), in relation to state-of-the-art satellite-based aerosol sensors (e.g., MODIS and MiSR) the major factor affecting the quality of aerosol products is sub-pixel cloud contamination. It is expected that TROPOMI's improved spatial resolution in relation to the heritage sensor (OMI), and the availability of a dedicated VIIRS-based will ameliorate sub-pixel cloud contamination effects.

In general, TROPOMAER retrievals are more reliable over land than over water surfaces. The near-UV retrieval method is particularly sensitive to carbonaceous and mineral aerosols. The sources of these aerosol types are located over the continents, and the atmospheric aerosol load associated with these events is generally large. In addition, dust and smoke aerosol events tend to take place under meteorological conditions which do not favor the formation of clouds in the vicinity of the sources, such as arid and semi-arid areas in the case of dust, and the dry season in the case of biomass burning.

Ocean TROPOMAER retrievals are affected by other factors. In addition to sub-pixel clouds, the ocean surface reflectance shows distinct angular and spectral variations (compared to land) due to spectrally varying scattering from the water, often called water-leaving radiances. (WLR), chlorophyll, sediments and other types of suspended matter decrease WLR. Spectral variations of ocean reflectance are accounted for making use of a climatology of wavelength dependent surface reflectance data set. Short-term variability, however, is not taken into account in the current version of the algorithm. Ocean retrievals of AOD and AAOD are not reported for sun glint angles smaller than 40º or for scenes where UVAI is less than 1.0.

The AOD over land is expected to have the same root mean square (rms) error as OMI retrievals (largest of 0.1 or 30%). The rms error in AOD over water is likely to be 2 times larger. The rms error for AAOD is estimated to be ~0.01.

For environments where sub-pixel cloud contamination is persistent during all seasons the statistics of the TROPOMAER-AERONET comparisons are poor. For these conditions comparisons over a longer period are needed to better assess the quality of the TROPOMI aerosol product.

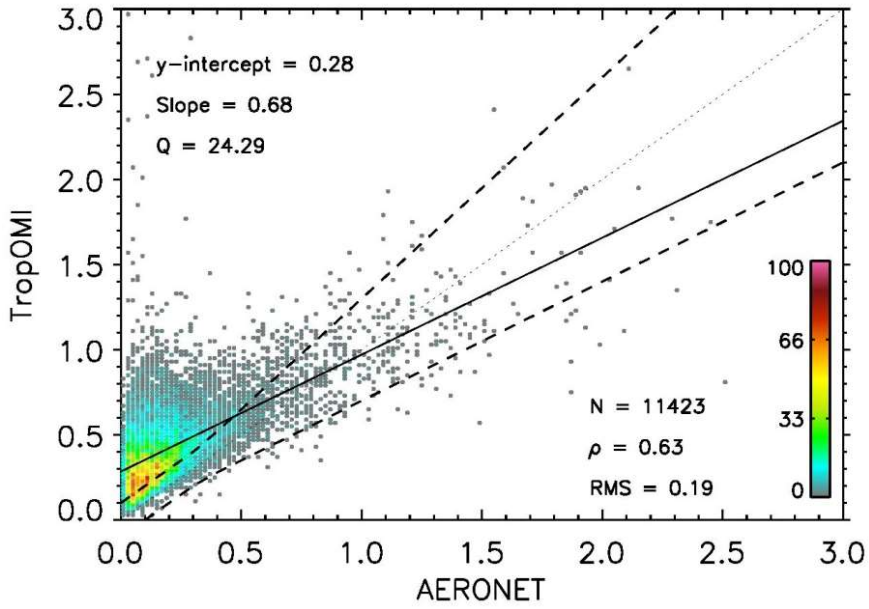

Figure 3. Scatter density plot of the TROPOMAER-AERONET comparison of daily aerosol optical depth over a total of 299 AERONET sites. Comparisons were done using all available AERONET retrievals for the period 2018-2019.

The TROPOMAER retrieved 388 nm single scattering albedo has been evaluated by comparison to AERONET retrievals at several sites. Figure 4 shows AERONET-TROPOMAER SSA comparisons. Comparisons were done using all available AERONET retrievals for the period 2018-2019. Because of the lack of AERONET near UV observations, the TROPOMI results have been converted to 440 nm to facilitate this analysis. Overall, TROPOMAER SSA retrievals agree reasonably well with AERONET results within 0.03 (dashed lines) and 0.05 (dotted lines).

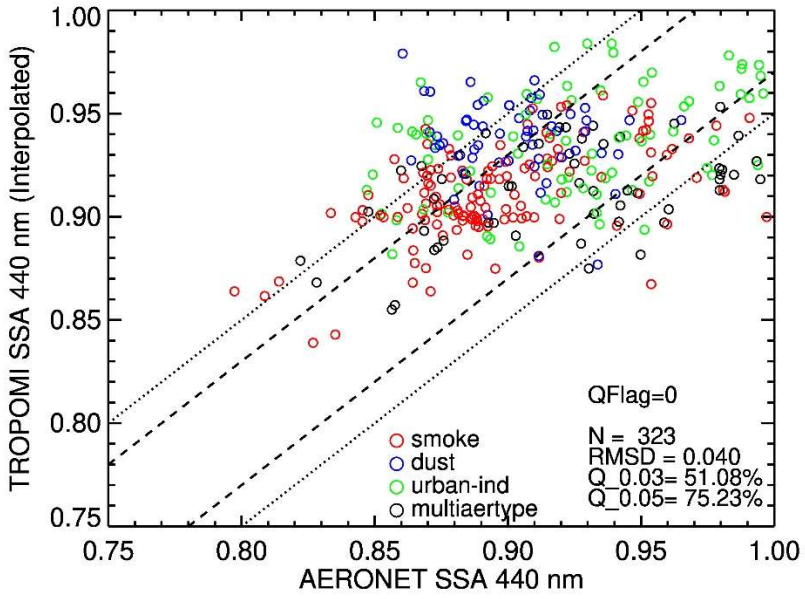

Figure 4. TROPOMAER-AERONET comparison of single scattering albedo.

4. Product Description

The TROPOMAER L2 data files are provided in the NetCDF4.0 format (Network Common Data Form Version 4.0, Unidata | NetCDF (ucar.edu)) These files use the data structure format that follows a specific file naming convention and dataset organization. Formats are "self-describing" with a header which describes the layout of the rest of the file, the data arrays, as well as arbitrary file metadata in the form of name/value attributes.

4.1. File naming convention

The components of file names are as follows:
TROPOMI-Sentinel-5P_L2-TROPOMAER_ observationDate-**o**ZZZZZ_vID-productionTime.**nc**

observationDate = start date of measurements in YYYY**m**MMDD format
- YYYY = 4-digit year number [2018-current]
- MM = 2-digit month number [01-12]
- DD = 2-digit day number [01-31]

ZZZZZ = 5-digit orbit number
vID = 2-digit collection number (01)
productionTime = file creation stamp in YYYY**m**MMDD**t**hhmmss format
- hhmmss= hour(hh), minute(mm), and second(ss) in local time

File name example:
TROPOMI-Sentinel-5P_L2-TROPOMAER_2021m0910t075921-o20259_v01-2021m0913t061126.nc

4.2. Data contents

The top-most level in the NetCDF4.0 of TROPOMAER L2 files contains two directories, one for each type of pixel-dependent data: GEODATA (containing data to geolocate each pixel, as well as viewing angle information), and SCIDATA (containing the calibrated radiances, AOD, SSA, AOD-above cloud, Reflectivity, and UVAI).

TROPOMAER L2 file includes the following dimension terms:

- ground_pixel = Across-track dimension (450)
- scanline = Along-track dimension (4172)
- WavelengthPair = Two wavelengths (354 and 388 nm)
- Wavelengths = Three wavelengths (354, 388, and 500 nm)
- layer = Five aerosol layer heights (0.0, 1.5., 3.0, 6.0, 10.0 km)
- ncorner = Latitude and Longitude corner bound dimension (4)

The key data fileds most likely to be used by typical users are listed below with path directories and dimensions:

/GEODATA/latitude	[4172, 450]
/GEODATA/latitude_bounds	[4172, 450, 4]
/GEODATA/longitude	[4172, 450]
/GEODATA/longitude_bounds	[4172, 450, 4]
/SCIDATA/AerosolAbsOpticalDepthVsHeight	[4172, 450, 5, 3]
/SCIDATA/AerosolCorrCloudOpticalDepth	[4172, 450]
/SCIDATA/AerosolOpticalDepthOverCloud	[4172, 450, 3]
/SCIDATA/AerosolOpticalDepthVsHeight	[4172, 450, 5, 3]
/SCIDATA/AerosolSingleScattAlbVsHeight	[4172, 450, 5, 3]
/SCIDATA/FinalAerosolAbsOpticalDepth	[4172, 450, 3]
/SCIDATA/FinalAerosolLayerHeight	[4172, 450]
/SCIDATA/FinalAerosolOpticalDepth	[4172, 450, 3]
/SCIDATA/FinalAerosolSingleScattAlb	[4172, 450, 3]
/SCIDATA/FinalAlgorithmFlags	[4172, 450]
/SCIDATA/FinalAlgorithmFlagsACA	[4172, 450]
/SCIDATA/NormRadiance	[4172, 450, 3]
/SCIDATA/Reflectivity	[4172, 450, 2]
/SCIDATA/Residue	[4172, 450]
/SCIDATA/UVAerosolIndex	[4172, 450]
/SCIDATA/VIIRS_confidently_clear	[4172, 450]

A complete list of the parameters with attributes for a sample file (TROPOMI-Sentinel-5P_L2-TROPOMAER_2021m0910t075921-o20259_v01-2021m0913t061126.nc) is given in APPENDIX 2.

Questions related to the TROPOMAER aerosol dataset should be directed to the GES DISC. For questions and comments related to the TROPOMAER aerosol algorithm and data quality, please contact Omar Torres (omar.o.torres@nasa.gov) who has the overall responsibility for these products.

References and related publications

Ahmad, Z., P. K. Bhartia, and N. Krotkov (2004), Spectral properties of backscattered UV radiation in cloudy atmospheres, J. Geophys. Res., 109, D01201, doi:10.1029/2003JD003395.

Ahn, C., O. Torres, and H. Jethva (2014), Assessment of OMI near-UV aerosol optical depth over land, J. Geophys. Res. Atmos., 119, 2457–2473, *doi:*10.1002/2013JD020188.

Ahn C., O. Torres, and P.K. Bhartia (2008), Comparison of OMI UV Aerosol Products with Aqua-MODIS and MISR observations in 2006, *J. Geophys. Res*, 113, D16S27, doi:10.1029/2007JD008832.

Chandrasekhar, S., Radiative Transfer, Dover, New York, 1960.

Cox, C., and W. Munk (1954) Measurement of the roughness of the sea surface from photographs of the Sun's glitter, J. Opt. Soc. Amer., 44, 838–850.

Dave, J.V., and C.L. Mateer (1967), A preliminary study on the possibility of estimating total atmospheric ozone from satellite measurements, *J. Atm Sci.,* 24, 414-427

Deirmendjian, D (1964), Scattering and polarization properties of water clouds and hazes in the visible and infrared, Appl. Opt., 3, 187–196.

Dubovik, O., *et al. (*2006*),* Application of spheroid models to account for aerosol particle nonsphericity in remote sensing of desert dust, *J. Geophys. Res.*, 111, *D11208, doi:*10.1029/2005JD006619.

Fromm, M., R. Bevilacqua, R. Servranckx, J. Rosen, J.P. Thayer, J. Herman, and D. Larko, Pyro-cumulonimbus injection of smoke to the stratosphere: Observations and impact of a super blowup in northwestern Canada on 3-4 August 1998, J. Geophys. Res.,110, doi:10.1029/2004JD005350, 2005

Gassó, S. and Torres, O.: The role of cloud contamination, aerosol layer height and aerosol model in the assessment of the OMI near-UV retrievals over the ocean, Atmos. Meas. Tech., 9, 3031-3052, doi:10.5194/amt-9-3031-2016, 2016

Ginoux, P., M. Chin, I. Tegen, J. Prospero, B. Holben, D. Dubovik,and S. J. Lin, 2001: Sources and distributions of dust aerosols simulated with the GOCART model. *J. Geophys. Res.,* **106,** 20,255–20,273.

Herman, J.R., and E. A. Celarier, Earth surface reflectivity climatology at 340 and 380 nm from TOMS data, J. Geophys. Res., 102, 28,003-28,011, 1997

IGBP, http://www-surf.larc.nasa.gov/surf/pages/sce_type.html

Jethva, H., O. Torres, and C. Ahn (2014), Global assessment of OMI aerosol single-scattering albedo using ground-based AERONET inversion, J. Geophys. Res. Atmos., 119, doi:10.1002/2014JD021672.

Jethva, H. and O. Torres (2011): Satellite-based evidence of wavelength-dependent aerosol absorption in biomass burning smoke inferred from ozone monitoring instrument, Atmos. Chem. Phys., 11, 10541-10551, doi:10.5194/acpd-11-7291-2011.

Jethva, H., O. Torres, and C. Ahn (2018), A12-year long global record of optical depth of absorbing aerosols above the clouds derived from the OMI/OMACA algorithm, Atmospheric Measurement Techniques, *11*, 5837–5864. https://doi.org/10.5194/amt-11-5837-2018

Joiner J. and A.P. Vasilkov, First Results From the OMI Rotational Raman Scattering Cloud Pressure Algorithm, IEEE Trans. Geo. Rem. Sens., 2006, Vol. **44**, No. 5, 1272-1282, doi:10.1109/TGRS.2005.861385.

Kleipool, Q. L., M. R. Dobber, J. F. de Haan, and P. F. Levelt (2008), Earth surface reflectance climatology from 3 years of OMI data, J. Geophys. Res., 113, D18308, doi:10.1029/2008JD010290.

Livingston,J.M, J. Redemann, P. B. Russell, O. Torres, B. Veihelmann, P. Veefkind, R. Braak, A. Smirnov, L. Remer, R. W. Bergstrom, O. Coddington, K. S. Schmidt, P. Pilewskie, R. Johnson, and Q. Zhang (2009), Comparison of aerosol optical depths from the Ozone Monitoring Instrument (OMI) on Aura with results from airborne sunphotometry, other space and ground measurements, Atmos. Chem. Phys. Discuss., 9, 6743-6765

McPeters, R. D., Bhartia, P. K., Krueger, A. J., Herman, J. R., Wellemeyer, C. G., Seftor, C. J., Jaross, G., Torres, O., Moy, L., Labow, G., Byerly, W., Taylor, S. L., Swissler, T., and Cebula, R. P (1998, Earth Probe Total Ozone Mapping Spectrometer (TOMS) Data Products User's Guide, NASA Technical Publication 1998-206895

Penning de Vries, M. and Wagner, T.: Modelled and measured effects of clouds on UV Aerosol Indices on a local, regional, and global scale, Atmos. Chem. Phys., 11, 12715-12735, doi:10.5194/acp-11-12715-2011, 2011.

Siddans, R.: S5P-NPP Cloud Processor ATBD, S5PNPPCRALATBD- 0001, available at: https://sentinel.esa.int/ web/sentinel/technical-guides/sentinel-5p/products-algorithms (last access: 2 December 2020), 2016.

Torres, O., Bhartia, P. K., Jethva, H., and Ahn, C. (2018). Impact of the ozone monitoring instrument row anomaly on the long-term record of aerosol products. *Atmospheric Measurement Techniques*, *11*, 2701–2715. https://doi.org/10.5194/amt-11-2701-2018

Torres, O., Ahn, C., and Chen, Z.: Improvements to the OMI near UV aerosol algorithm using A-train CALIOP and AIRS observations, Atmos. Meas. Tech., 6, 5621-5652, doi:10.5194/amtd-6-5621-2013, 2013.

Torres, O., A. Tanskanen, B. Veihelman, C. Ahn, R. Braak, P. K. Bhartia, P. Veefkind, and P. Levelt (2007), Aerosols and Surface UV Products from OMI Observations: An Overview, *J. Geophys. Res.,* 112, D24S47, doi:10.1029/2007JD008809.

Torres O., P.K. Bhartia, J.R. Herman and Z. Ahmad, Derivation of aerosol properties from satellite measurements of backscattered ultraviolet radiation. Theoretical Basis, J. Geophys. Res., 103, 17099-17110, 1998

Torres, O., P.K. Bhartia, A. Syniuk, and E. Welton, TOMS Measurements of Aerosol Absorption from Space: Comparison to SAFARI 2000 Ground based Observations, J. Geophys. Res., 110, D10S18, doi:10.10129/2004JD004611, 2005

Torres, O., Jethva, H., Ahn, C., Jaross, G., and Loyola, D.G., (2020), TROPOMI Aerosol Products: Evaluation and Observations of Synoptic Scale Carbonaceous Aerosol Plumes during 2018-2020, Atmos. Meas. Tech., 13, 6789–6806, 2020 https://doi.org/10.5194/amt-13-6789-202.

APPENDIX 1

OMI CRB AEROSOL MODELS

Real refractive index 1.50 (wavelength independent)

Models 1:4

R_F	R_C	σ_F	σ_C	Fraction
0.08	0.705	1.492	2.075	$2.05\ 10^{-4}$

Nodal points on imaginary refractive index (wavelength dependent):
354.0 nm: 0.0576, 0.0480, 0.0360, 0.0240
388.0 nm: 0.0480, 0.0400, 0.0300, 0.0200

Models 5:7

R_F	R_C	σ_F	σ_C	Fraction
0.087	0.567	1.537	2.203	$2.06\ 10^{-4}$

Nodal points on imaginary refractive index (wavelength dependent):
354.0 nm: 0.01200, 0.0060, 0.00000
388.0 nm: 0.01000, 0.0050, 0.00000

OMI SLF AEROSOL MODELS

Models 1:7

Real refractive index 1.40 (wavelength independent)

R_F	R_C	σ_F	σ_C	Fraction
0.088	0.509	1.499	2.160	$4.04\ 10^{-4}$

Nodal points on imaginary refractive index (wavelength dependent):
354.0 nm: 0.03600, 0.03000, 0.02400, 0.01800, 0.01200, 0.00600, 0.00000
388.0 nm: 0.03000, 0.02500, 0.02000, 0.01500, 0.01000, 0.00500, 0.00000

OMI DST AEROSOL MODELS

Real refractive index 1.55 (wavelength independent)

Models 1:7

R_F	R_C	σ_F	σ_C	Fraction
0.052	0.67	1.697	1.806	$4.35\ 10^{-3}$

Nodal points on imaginary refractive index (wavelength dependent):

354.0 nm: 0.02303, 0.01279, 0.00832, 0.00561, 0.00256, 0.00128, 0.00000
388.0 nm: 0.01662, 0.00923, 0.00600, 0.00405, 0.00185, 0.00092, 0.00000

R_F & R_c are radii for fine and coarse mode aerosols
$\sigma_{F\ \&}\ \sigma_C$ are the standard deviations

The table below describes the distribution of spheroid axis ratio and associated weights assumed in the calculation of DST models phase function. Note that the fraction weights sum up to 1.00.

Axis Ratio	Fractional Weight
0.33490	0.0661850
0.36690	0.0650250
0.40190	0.0636350
0.44030	0.0620500
0.48230	0.0587200
0.52830	0.0533500
0.57870	0.0477625
0.63390	0.0429530
0.69440	0.0403205
0.76070	0.0000000
0.83330	0.0000000
0.91290	0.0000000
1.00000	0.0000000
1.09540	0.0000000
1.20000	0.0000000
1.31450	0.0000000
1.44000	0.0403205
1.57740	0.0429530
1.72800	0.0477625
1.89290	0.0533500
2.07360	0.0587200
2.27150	0.0620500
2.48832	0.0636350
2.72580	0.0650250
2.98600	0.0661850

APPENDIX 2

```
netcdf TROPOMI-Sentinel-5P_L2-TROPOMAER_2021m0910t075921-o20259_v01-2021m0913t061126 {
dimensions:
        scanline = 4172 ;
        ground_pixel = 450 ;
        ncorner = 4 ;
        WavelengthPair = 2 ;
        Wavelengths = 3 ;
        layer = 5 ;
variables:
        float WavelengthPair(WavelengthPair) ;
                WavelengthPair:units = "nm" ;
        float Wavelengths(Wavelengths) ;
                Wavelengths:units = "nm" ;
        float layer(layer) ;
                layer:units = "km" ;
        int scanline(scanline) ;
        int ground_pixel(ground_pixel) ;
        int ncorner(ncorner) ;

// global attributes:
                :time_coverage_start = "2021-09-10T08:20:56Z" ;
                :time_coverage_end = "2021-09-10T09:19:19Z" ;
                :time_reference = "2021-09-10T00:00:00Z" ;
                :VersionID = "1" ;
                :DataSetQuality = "Excellent data quality" ;
                :OrbitNumber = 20259 ;
                :orbit = 20259 ;
                :PGEVersion = "1.1.1" ;
                :history = "2021-09-13T06:11:25Z; APPVersion=1.1.1" ;
                :ProcessingCenter = "OZONE PEATE" ;
                :ProcessingHost = "Linux minion7087 3.10.0-1160.36.2.el7.x86_64 x86_64" ;
                :ProcessingLevel = "2" ;
                :Conventions = "CF-1.6" ;
                :institution = "NASA/GSFC" ;
                :LocalGranuleID = "TROPOMI-Sentinel-5P_L2-TROPOMAER_2021m0910t075921-o20259_v01-2021m0913t061125.nc" ;
                :source = "Sentinel 5 Precursor" ;
                :identifier_product_doi = "10.5067/MEASURES/AER/DATA204" ;
                :identifier_product_doi_authority = "https://dx.doi.org/" ;
                :references = "Torres, O., Jethva, H., Ahn, C., Jaross, G., and Loyola, D.G., (2020), TROPOMI Aerosol Products: Evaluation and Observations of Synoptic Scale Carbonaceous Aerosol Plumes during 2018-2020, Atmos. Meas. Tech., 13, 6789–6806, 2020 https://doi.org/10.5194/amt-13-6789-202." ;
```

:Format = "netCDF-4" ;
:PlatformShortName = "Sentinel-5P" ;
:InstrumentShortName = "TROPOMI" ;
:NumTimes = 4172 ;
:ProductionDateTime = "2021-09-13T06:11:25Z" ;
:ShortName = "TROPOMAER" ;
:title = "TROPOMI/Sentinel-5P Near UV Aerosol Optical Depth and Single Scattering Albedo L2 1-Orbit Snapshot 7.5 km x 3 km" ;
:comment = "" ;
:AuthorAffiliation = "NASA-GSFC" ;
:AuthorName = "Omar Torres" ;
data:

WavelengthPair = 354, 388 ;

Wavelengths = 354, 388, 500 ;

layer = 0, 1.5, 3, 6, 10 ;

scanline = 1 - 4172 ;

ground_pixel = 1- 450 ;

ncorner = 1, 2, 3, 4 ;

group: GEODATA {
variables:
float latitude(scanline, ground_pixel) ;
latitude:comment = "Latitude of the center of each ground pixel on the WGS84 reference ellipsoid" ;
latitude:_FillValue = 9.96921e+36f ;
latitude:long_name = "pixel center latitude" ;
latitude:max_val = 90.f ;
latitude:min_val = -90.f ;
latitude:standard_name = "latitude" ;
latitude:units = "degrees_north" ;
latitude:bounds = "/GEODATA/latitude_bounds" ;
float longitude(scanline, ground_pixel) ;
longitude:comment = "Longitude of the center of each ground pixel on the WGS84 reference ellipsoid" ;
longitude:_FillValue = 9.96921e+36f ;
longitude:long_name = "pixel center longitude" ;
longitude:max_val = 180.f ;
longitude:min_val = -180.f ;
longitude:standard_name = "longitude" ;
longitude:units = "degrees_east" ;

longitude:bounds = "/GEODATA/longitude_bounds" ;
float latitude_bounds(scanline, ground_pixel, ncorner) ;
latitude_bounds:comment = "The four latitude boundaries of each ground pixel." ;
latitude_bounds:_FillValue = 9.96921e+36f ;
latitude_bounds:units = "degrees_north" ;
float longitude_bounds(scanline, ground_pixel, ncorner) ;
longitude_bounds:comment = "The four longitude boundaries of each ground pixel." ;
longitude_bounds:_FillValue = 9.96921e+36f ;
longitude_bounds:units = "degrees_east" ;
float satellite_altitude(scanline) ;
satellite_altitude:comment = "The altitude of the spacecraft relative to the WGS84 reference ellipsoid" ;
satellite_altitude:_FillValue = 9.96921e+36f ;
satellite_altitude:long_name = "satellite altitude" ;
satellite_altitude:max_val = 900000.f ;
satellite_altitude:min_val = 700000.f ;
satellite_altitude:units = "m" ;
float satellite_latitude(scanline) ;
satellite_latitude:comment = "Latitude of the spacecraft sub-satellite point on the WGS84 reference ellipsoid" ;
satellite_latitude:_FillValue = 9.96921e+36f ;
satellite_latitude:long_name = "sub-satellite latitude" ;
satellite_latitude:max_val = 90.f ;
satellite_latitude:min_val = -90.f ;
satellite_latitude:units = "degrees_north" ;
float satellite_longitude(scanline) ;
satellite_longitude:comment = "Longitude of the spacecraft sub-satellite point on the WGS84 reference ellipsoid" ;
satellite_longitude:_FillValue = 9.96921e+36f ;
satellite_longitude:max_val = 180.f ;
satellite_longitude:min_val = -180.f ;
satellite_longitude:units = "degrees_east" ;
float viewing_zenith_angle(scanline, ground_pixel) ;
viewing_zenith_angle:comment = "Zenith angle of the satellite at the ground pixel location on the reference ellipsoid. Angle is measured away from the vertical." ;
viewing_zenith_angle:_FillValue = 9.96921e+36f ;
viewing_zenith_angle:long_name = "viewing zenith angle" ;
viewing_zenith_angle:max_val = 180.f ;
viewing_zenith_angle:min_val = 0.f ;
viewing_zenith_angle:units = "degree" ;
viewing_zenith_angle:standard_name = "platform_zenith_angle" ;
viewing_zenith_angle:coordinates = "/GEODATA/longitude /GEODATA/latitude" ;
float viewing_azimuth_angle(scanline, ground_pixel) ;

viewing_azimuth_angle:comment = "Azimuth angle of the satellite at the ground pixel location on the reference ellipsoid. Angle is measured clockwise from the North (East = +90, South = -+180, West = -90)" ;
viewing_azimuth_angle:_FillValue = 9.96921e+36f ;
viewing_azimuth_angle:units = "degree" ;
viewing_azimuth_angle:long_name = "viewing azimuth angle" ;
viewing_azimuth_angle:standard_name = "platform_azimuth_angle" ;
viewing_azimuth_angle:max_val = 180.f ;
viewing_azimuth_angle:min_val = -180.f ;
viewing_azimuth_angle:coordinates = "/GEODATA/longitude /GEODATA/latitude" ;
float solar_zenith_angle(scanline, ground_pixel) ;
solar_zenith_angle:comment = "Solar zenith angle at the ground pixel location on the reference ellipsoid. Angle is measured away from the vertical. ESA definition of day side: SZA less the 92 degrees" ;
solar_zenith_angle:_FillValue = 9.96921e+36f ;
solar_zenith_angle:long_name = "solar zenith angle" ;
solar_zenith_angle:standard_name = "solar_zenith_angle" ;
solar_zenith_angle:max_val = 180.f ;
solar_zenith_angle:min_val = 0.f ;
solar_zenith_angle:units = "degree" ;
solar_zenith_angle:coordinates = "/GEODATA/longitude /GEODATA/latitude" ;
float solar_azimuth_angle(scanline, ground_pixel) ;
solar_azimuth_angle:comment = "Solar azimuth angle at the ground pixel location on the reference ellipsoid. Angle is measured clockwise from the North (East = +90, South = -+180, West = -90)" ;
solar_azimuth_angle:_FillValue = 9.96921e+36f ;
solar_azimuth_angle:long_name = "solar azimuth angle" ;
solar_azimuth_angle:max_val = 180.f ;
solar_azimuth_angle:min_val = -180.f ;
solar_azimuth_angle:standard_name = "solar_azimuth_angle" ;
solar_azimuth_angle:units = "degree" ;
solar_azimuth_angle:coordinates = "/GEODATA/longitude /GEODATA/latitude" ;
int time ;
time:comment = "Reference time of the measurements. The reference time is set to yyyy-mm-ddT00:00:00 UTC, where yyyy-mm-dd is the day on which the measurements of a particular data granule start." ;
time:long_name = "reference start time of measurement" ;
time:standard_name = "time" ;
time:units = "seconds since 2010-01-01 00:00:00" ;
int delta_time(scanline) ;
delta_time:comment = "Time difference with time for each measurement" ;
delta_time:_FillValue = -2147483647 ;
delta_time:long_name = "offset from the reference start time of measurement" ;

```
            delta_time:units = "milliseconds since 2021-09-10 00:00:00" ;
        float RelativeAzimuthAngle(scanline, ground_pixel) ;
            RelativeAzimuthAngle:units = "deg(EastofNorth)" ;
            RelativeAzimuthAngle:long_name = "Relative (sun + 180 - view) Azimuth
Angle (deg)" ;
            RelativeAzimuthAngle:coordinates = "/GEODATA/longitude
/GEODATA/latitude" ;
            RelativeAzimuthAngle:_FillValue = -1.267651e+30f ;
            RelativeAzimuthAngle:valid_min = -180.f ;
            RelativeAzimuthAngle:valid_max = 180.f ;
        float SnowIce_Fraction(scanline, ground_pixel) ;
            SnowIce_Fraction:units = "1" ;
            SnowIce_Fraction:long_name = "Snow Ice Fraction" ;
            SnowIce_Fraction:coordinates = "/GEODATA/longitude /GEODATA/latitude"
;
            SnowIce_Fraction:_FillValue = -1.267651e+30f ;
            SnowIce_Fraction:valid_min = 0.f ;
            SnowIce_Fraction:valid_max = 100.f ;
        float TerrainPressure(scanline, ground_pixel) ;
            TerrainPressure:units = "hPa" ;
            TerrainPressure:long_name = "Terrain Pressure" ;
            TerrainPressure:coordinates = "/GEODATA/longitude /GEODATA/latitude" ;
            TerrainPressure:_FillValue = -1.267651e+30f ;
            TerrainPressure:valid_min = 0.f ;
            TerrainPressure:valid_max = 1013.f ;
 data:
 } // group GEODATA

group: SCIDATA {
 variables:
        ubyte AIRSCO_Flags(scanline, ground_pixel) ;
            AIRSCO_Flags:units = "1" ;
            AIRSCO_Flags:long_name = "AIRSCO_Flags" ;
            AIRSCO_Flags:coordinates = "/GEODATA/longitude /GEODATA/latitude" ;
            AIRSCO_Flags:flag_meanings = "Today_AIRS_CO_L-3_file
Yesterday_AIRS_CO_L-3_file Climatology" ;
            AIRSCO_Flags:_FillValue = 255UB ;
            AIRSCO_Flags:valid_min = 1UB ;
            AIRSCO_Flags:valid_max = 3UB ;
            AIRSCO_Flags:flag_values = 1UB, 2UB, 3UB ;
        float AIRSL3COvalue(scanline, ground_pixel) ;
            AIRSL3COvalue:units = "molecules/cm^2" ;
            AIRSL3COvalue:long_name = "AIRS CO L3 data" ;
            AIRSL3COvalue:coordinates = "/GEODATA/longitude /GEODATA/latitude" ;
            AIRSL3COvalue:_FillValue = -9999.f ;
            AIRSL3COvalue:valid_min = 0.f ;
```

AIRSL3COvalue:valid_max = 5.e+18f ;
float AerosolAbsOpticalDepthVsHeight(scanline, ground_pixel, layer, Wavelengths) ;
AerosolAbsOpticalDepthVsHeight:units = "1" ;
AerosolAbsOpticalDepthVsHeight:long_name = "Aerosol Absorption Optical Depth at 5 levels" ;
AerosolAbsOpticalDepthVsHeight:coordinates = "/GEODATA/longitude /GEODATA/latitude /layer /Wavelengths" ;
AerosolAbsOpticalDepthVsHeight:_FillValue = -1.267651e+30f ;
AerosolAbsOpticalDepthVsHeight:valid_min = 0.f ;
AerosolAbsOpticalDepthVsHeight:valid_max = 4.f ;
float AerosolOpticalDepthVsHeight(scanline, ground_pixel, layer, Wavelengths) ;
AerosolOpticalDepthVsHeight:units = "1" ;
AerosolOpticalDepthVsHeight:long_name = "Aerosol Optical Depth at 5 levels" ;
AerosolOpticalDepthVsHeight:coordinates = "/GEODATA/longitude /GEODATA/latitude /layer /Wavelengths" ;
AerosolOpticalDepthVsHeight:_FillValue = -1.267651e+30f ;
AerosolOpticalDepthVsHeight:valid_min = 0.f ;
AerosolOpticalDepthVsHeight:valid_max = 10.f ;
float AerosolSingleScattAlbVsHeight(scanline, ground_pixel, layer, Wavelengths) ;
AerosolSingleScattAlbVsHeight:units = "1" ;
AerosolSingleScattAlbVsHeight:long_name = "Aerosol Single Scattering Albedo at 5 levels" ;
AerosolSingleScattAlbVsHeight:coordinates = "/GEODATA/longitude /GEODATA/latitude /layer /Wavelengths" ;
AerosolSingleScattAlbVsHeight:_FillValue = -1.267651e+30f ;
AerosolSingleScattAlbVsHeight:valid_min = 0.f ;
AerosolSingleScattAlbVsHeight:valid_max = 1.f ;
ubyte AerosolType(scanline, ground_pixel) ;
AerosolType:units = "1" ;
AerosolType:long_name = "Aerosol Type" ;
AerosolType:coordinates = "/GEODATA/longitude /GEODATA/latitude" ;
AerosolType:flag_meanings = "smoke dust urban/industrial_pollutant unknown" ;
AerosolType:comment = "Aerosol types identified with a combination of AIRS CO, UVAI, and surface types" ;
AerosolType:_FillValue = 255UB ;
AerosolType:valid_min = 1UB ;
AerosolType:valid_max = 3UB ;
AerosolType:flag_values = 1UB, 2UB, 3UB, 255UB ;
ushort AlgorithmFlagsVsHeight(scanline, ground_pixel, layer) ;
AlgorithmFlagsVsHeight:units = "1" ;
AlgorithmFlagsVsHeight:long_name = "Algorithm Flags Vs Height" ;
AlgorithmFlagsVsHeight:coordinates = "/GEODATA/longitude /GEODATA/latitude /layer" ;

AlgorithmFlagsVsHeight:flag_meanings = "most_reliable less_reliable unused out-of-bounds_SSA_or_AOD_above_6.0_at_500nm cloud/snow/ice_contaminated_data solar_zenith_angle_above_threshold(70_degrees) sun_glint_angle_below_thresold_over_water(40_degrees) Terrain_Pressure_below_threshold(250_hPa)" ;
AlgorithmFlagsVsHeight:_FillValue = 65535US ;
AlgorithmFlagsVsHeight:valid_min = 0US ;
AlgorithmFlagsVsHeight:valid_max = 8US ;
AlgorithmFlagsVsHeight:flag_values = 0US, 1US, 2US, 3US, 4US, 5US, 6US, 7US ;
ushort AlgorithmFlags_AerosolIndex(scanline, ground_pixel) ;
AlgorithmFlags_AerosolIndex:units = "1" ;
AlgorithmFlags_AerosolIndex:long_name = "Algorithm Flags for AerosolIndex" ;
AlgorithmFlags_AerosolIndex:coordinates = "/GEODATA/longitude /GEODATA/latitude" ;
AlgorithmFlags_AerosolIndex:flag_meanings = "Glint_angles_less_than_20 degree Cloud_fraction_less_than_0.0 Cloud_fraction_equal_to_1.0 Snow/ice_covered_pixels Cloud_optical_depth_equal_to_100.0" ;
AlgorithmFlags_AerosolIndex:_FillValue = 65535US ;
AlgorithmFlags_AerosolIndex:valid_min = 0US ;
AlgorithmFlags_AerosolIndex:valid_max = 4US ;
AlgorithmFlags_AerosolIndex:flag_masks = 1US, 2US, 4US, 8US, 16US ;
float CloudFraction(scanline, ground_pixel) ;
CloudFraction:units = "1" ;
CloudFraction:long_name = "Cloud Fraction" ;
CloudFraction:coordinates = "/GEODATA/longitude /GEODATA/latitude" ;
CloudFraction:_FillValue = -1.267651e+30f ;
CloudFraction:valid_min = 0.f ;
CloudFraction:valid_max = 1.f ;
float CloudOpticalDepth(scanline, ground_pixel) ;
CloudOpticalDepth:units = "1" ;
CloudOpticalDepth:long_name = "Cloud Optical Depth" ;
CloudOpticalDepth:coordinates = "/GEODATA/longitude /GEODATA/latitude" ;
CloudOpticalDepth:_FillValue = -1.267651e+30f ;
CloudOpticalDepth:valid_min = 0.f ;
CloudOpticalDepth:valid_max = 100.f ;
float ApparentCloudOpticalDepth(scanline, ground_pixel) ;
ApparentCloudOpticalDepth:units = "1" ;
ApparentCloudOpticalDepth:long_name = "Apparent Cloud Optical Depth" ;
ApparentCloudOpticalDepth:coordinates = "/GEODATA/longitude /GEODATA/latitude" ;
ApparentCloudOpticalDepth:_FillValue = -1.267651e+30f ;
ApparentCloudOpticalDepth:valid_min = 0.f ;
ApparentCloudOpticalDepth:valid_max = 100.f ;

float AerosolCorrCloudOpticalDepth(scanline, ground_pixel) ;
AerosolCorrCloudOpticalDepth:units = "1" ;
AerosolCorrCloudOpticalDepth:long_name = "Aerosol Corrected Cloud Optical Depth" ;
AerosolCorrCloudOpticalDepth:coordinates = "/GEODATA/longitude /GEODATA/latitude" ;
AerosolCorrCloudOpticalDepth:_FillValue = -1.267651e+30f ;
AerosolCorrCloudOpticalDepth:valid_min = 0.f ;
AerosolCorrCloudOpticalDepth:valid_max = 100.f ;
float FinalAerosolAbsOpticalDepth(scanline, ground_pixel, Wavelengths) ;
FinalAerosolAbsOpticalDepth:units = "1" ;
FinalAerosolAbsOpticalDepth:long_name = "Best Aerosol Absorption Optical Depth" ;
FinalAerosolAbsOpticalDepth:coordinates = "/GEODATA/longitude /GEODATA/latitude /Wavelengths" ;
FinalAerosolAbsOpticalDepth:_FillValue = -1.267651e+30f ;
FinalAerosolAbsOpticalDepth:valid_min = 0.f ;
FinalAerosolAbsOpticalDepth:valid_max = 4.f ;
float AerosolOpticalDepthOverCloud(scanline, ground_pixel, Wavelengths) ;
AerosolOpticalDepthOverCloud:units = "1" ;
AerosolOpticalDepthOverCloud:long_name = "Aerosol Optical Depth Over Cloud" ;
AerosolOpticalDepthOverCloud:coordinates = "/GEODATA/longitude /GEODATA/latitude /Wavelengths" ;
AerosolOpticalDepthOverCloud:_FillValue = -1.267651e+30f ;
AerosolOpticalDepthOverCloud:valid_min = 0.f ;
AerosolOpticalDepthOverCloud:valid_max = 10.f ;
float FinalAerosolLayerHeight(scanline, ground_pixel) ;
FinalAerosolLayerHeight:units = "km" ;
FinalAerosolLayerHeight:long_name = "Final Aerosol Layer Height (km)" ;
FinalAerosolLayerHeight:coordinates = "/GEODATA/longitude /GEODATA/latitude" ;
FinalAerosolLayerHeight:_FillValue = -1.267651e+30f ;
FinalAerosolLayerHeight:valid_min = 0.f ;
FinalAerosolLayerHeight:valid_max = 10.f ;
float FinalAerosolOpticalDepth(scanline, ground_pixel, Wavelengths) ;
FinalAerosolOpticalDepth:units = "1" ;
FinalAerosolOpticalDepth:long_name = "Best Aerosol Optical Depth" ;
FinalAerosolOpticalDepth:coordinates = "/GEODATA/longitude /GEODATA/latitude /Wavelengths" ;
FinalAerosolOpticalDepth:_FillValue = -1.267651e+30f ;
FinalAerosolOpticalDepth:valid_min = 0.f ;
FinalAerosolOpticalDepth:valid_max = 10.f ;
float FinalAerosolSingleScattAlb(scanline, ground_pixel, Wavelengths) ;
FinalAerosolSingleScattAlb:units = "1" ;

FinalAerosolSingleScattAlb:long_name = "Best Aerosol Single Scattering Albedo" ;
FinalAerosolSingleScattAlb:coordinates = "/GEODATA/longitude /GEODATA/latitude /Wavelengths" ;
FinalAerosolSingleScattAlb:_FillValue = -1.267651e+30f ;
FinalAerosolSingleScattAlb:valid_min = 0.f ;
FinalAerosolSingleScattAlb:valid_max = 1.f ;
float InputAerosolSingleScattAlbACA(scanline, ground_pixel, Wavelengths) ;
InputAerosolSingleScattAlbACA:units = "1" ;
InputAerosolSingleScattAlbACA:long_name = "Input Aerosol Single-scattering Albedo" ;
InputAerosolSingleScattAlbACA:coordinates = "/GEODATA/longitude /GEODATA/latitude /Wavelengths" ;
InputAerosolSingleScattAlbACA:_FillValue = -1.267651e+30f ;
InputAerosolSingleScattAlbACA:valid_min = 0.f ;
InputAerosolSingleScattAlbACA:valid_max = 1.f ;
ushort FinalAlgorithmFlags(scanline, ground_pixel) ;
FinalAlgorithmFlags:units = "1" ;
FinalAlgorithmFlags:long_name = "Final Algorithm Flags" ;
FinalAlgorithmFlags:coordinates = "/GEODATA/longitude /GEODATA/latitude" ;
FinalAlgorithmFlags:flag_meanings = "most_reliable less_reliable unused out-of-bounds_SSA_or_AOD_above_6.0_at_500nm cloud/snow/ice_contaminated_data solar_zenith_angle_above_threshold(70_degrees) sun_glint_angle_below_thresold_over_water(40_degrees) Terrain_Pressure_below_threshold(250_hPa)" ;
FinalAlgorithmFlags:_FillValue = 65535US ;
FinalAlgorithmFlags:valid_min = 0US ;
FinalAlgorithmFlags:valid_max = 8US ;
FinalAlgorithmFlags:flag_values = 0US, 1US, 2US, 3US, 4US, 5US, 6US, 7US ;
ushort FinalAlgorithmFlagsACA(scanline, ground_pixel) ;
FinalAlgorithmFlagsACA:units = "1" ;
FinalAlgorithmFlagsACA:long_name = "Final Algorithm Flags for Above Cloud Aerosol retrievals" ;
FinalAlgorithmFlagsACA:coordinates = "/GEODATA/longitude /GEODATA/latitude" ;
FinalAlgorithmFlagsACA:comment = "for flag values and meanings see the README file" ;
FinalAlgorithmFlagsACA:_FillValue = 65535US ;
FinalAlgorithmFlagsACA:valid_min = 0US ;
FinalAlgorithmFlagsACA:valid_max = 8US ;
float FinalImRefIdx(scanline, ground_pixel, WavelengthPair) ;
FinalImRefIdx:units = "1" ;
FinalImRefIdx:long_name = "Final Imaginary Refractive Index" ;

FinalImRefIdx:coordinates = "/GEODATA/longitude /GEODATA/latitude /WavelengthPair" ;
FinalImRefIdx:_FillValue = -1.267651e+30f ;
FinalImRefIdx:valid_min = 0.f ;
FinalImRefIdx:valid_max = 1.f ;
float UncertaintyACAODToSSA(scanline, ground_pixel, WavelengthPair) ;
UncertaintyACAODToSSA:units = "1" ;
UncertaintyACAODToSSA:long_name = "Percent uncertainty in COD due to Change in SSA" ;
UncertaintyACAODToSSA:coordinates = "/GEODATA/longitude /GEODATA/latitude /WavelengthPair" ;
UncertaintyACAODToSSA:_FillValue = -1.267651e+30f ;
UncertaintyACAODToSSA:valid_min = -99.f ;
UncertaintyACAODToSSA:valid_max = 99.f ;
float UncertaintyCODToSSA(scanline, ground_pixel, WavelengthPair) ;
UncertaintyCODToSSA:units = "1" ;
UncertaintyCODToSSA:long_name = "Percent uncertainty in Aerosol-corrected COD due to plus/minus 0.03 change in SSA" ;
UncertaintyCODToSSA:coordinates = "/GEODATA/longitude /GEODATA/latitude /WavelengthPair" ;
UncertaintyCODToSSA:_FillValue = -1.267651e+30f ;
UncertaintyCODToSSA:valid_min = -99.f ;
UncertaintyCODToSSA:valid_max = 99.f ;
ubyte HeightFlags(scanline, ground_pixel) ;
HeightFlags:units = "1" ;
HeightFlags:long_name = "Height Flags" ;
HeightFlags:coordinates = "/GEODATA/longitude /GEODATA/latitude" ;
HeightFlags:flag_meanings = "CALIOP_climatology GOCART_climatology interpolated_in_between_3-6_km_within_+/-_30_–_45-degree_latitudes Assumed_height" ;
HeightFlags:comment = "sources of the prescribed aerosol layer height used in retrieving processes" ;
HeightFlags:_FillValue = 255UB ;
HeightFlags:valid_min = 1UB ;
HeightFlags:valid_max = 4UB ;
HeightFlags:flag_values = 1UB, 2UB, 3UB, 4UB ;
float ImaRefractiveIndex(scanline, ground_pixel, layer, Wavelengths) ;
ImaRefractiveIndex:units = "1" ;
ImaRefractiveIndex:long_name = "Imaginary refractive Index" ;
ImaRefractiveIndex:coordinates = "/GEODATA/longitude /GEODATA/latitude /layer /Wavelengths" ;
ImaRefractiveIndex:_FillValue = -1.267651e+30f ;
ImaRefractiveIndex:valid_min = 0.f ;
ImaRefractiveIndex:valid_max = 1.f ;
ushort MeasurementQualityFlags(scanline) ;
MeasurementQualityFlags:units = "1" ;

MeasurementQualityFlags:long_name = "Measurement Quality Flags" ;
MeasurementQualityFlags:flag_meanings = "no_error proc_skipped no_residual saa spacecraft_manoeuvre sub_grp irr_out_of_range sub_group" ;
MeasurementQualityFlags:comment = "Overall quality information for a measurement" ;
MeasurementQualityFlags:_FillValue = 65535US ;
MeasurementQualityFlags:valid_min = 0US ;
MeasurementQualityFlags:valid_max = 65534US ;
float NormRadiance(scanline, ground_pixel, Wavelengths) ;
NormRadiance:units = "1" ;
NormRadiance:long_name = "Normalized Radiance" ;
NormRadiance:coordinates = "/GEODATA/longitude /GEODATA/latitude /Wavelengths" ;
NormRadiance:_FillValue = -1.267651e+30f ;
NormRadiance:valid_min = 0.f ;
NormRadiance:valid_max = 1.f ;
float Reflectivity(scanline, ground_pixel, WavelengthPair) ;
Reflectivity:units = "1" ;
Reflectivity:long_name = "Lambert Equivalent Reflectivity" ;
Reflectivity:coordinates = "/GEODATA/longitude /GEODATA/latitude /WavelengthPair" ;
Reflectivity:_FillValue = -1.267651e+30f ;
Reflectivity:valid_min = 0.f ;
Reflectivity:valid_max = 1.f ;
float Radiance(scanline, ground_pixel, WavelengthPair) ;
Radiance:units = "mol.m-2.nm-1.s-1" ;
Radiance:long_name = "spectral photon radiance" ;
Radiance:coordinates = "/GEODATA/longitude /GEODATA/latitude /WavelengthPair" ;
Radiance:comment = "Measured spectral radiance for each spectral pixel" ;
Radiance:_FillValue = -1.267651e+30f ;
float Irradiance(ground_pixel, WavelengthPair) ;
Irradiance:units = "mol.m-2.nm-1.sr-1.s-1" ;
Irradiance:long_name = "spectral photon irradiance" ;
Irradiance:coordinates = "/GEODATA/longitude /WavelengthPair" ;
Irradiance:comment = "Measured spectral irradiance for each spectral pixel" ;
Irradiance:_FillValue = 9.96921e+36f ;
float ice_error(ground_pixel, WavelengthPair) ;
ice_error:units = "1" ;
ice_error:long_name = "Ice error" ;
ice_error:comment = "Reflectance correction factors as a function of cross-track positions for each wavelength, derived from the ice reflectance analysis" ;
ice_error:_FillValue = -1.267651e+30f ;
ice_error:valid_min = 0.f ;
ice_error:valid_max = 2.f ;
float Residue(scanline, ground_pixel) ;

Residue:units = "1" ;
Residue:long_name = "Residue" ;
Residue:coordinates = "/GEODATA/longitude /GEODATA/latitude" ;
Residue:_FillValue = -1.267651e+30f ;
Residue:valid_min = -10.f ;
Residue:valid_max = 30.f ;
float SurfaceAlbedo(scanline, ground_pixel, Wavelengths) ;
SurfaceAlbedo:units = "1" ;
SurfaceAlbedo:long_name = "Surface Albedo" ;
SurfaceAlbedo:coordinates = "/GEODATA/longitude /GEODATA/latitude /Wavelengths" ;
SurfaceAlbedo:_FillValue = -1.267651e+30f ;
SurfaceAlbedo:valid_min = 0.f ;
SurfaceAlbedo:valid_max = 1.f ;
float UVAerosolIndex(scanline, ground_pixel) ;
UVAerosolIndex:units = "1" ;
UVAerosolIndex:long_name = "UV Aerosol Index" ;
UVAerosolIndex:coordinates = "/GEODATA/longitude /GEODATA/latitude" ;
UVAerosolIndex:_FillValue = -1.267651e+30f ;
UVAerosolIndex:valid_min = -10.f ;
UVAerosolIndex:valid_max = 30.f ;
ushort SurfaceType(scanline, ground_pixel) ;
SurfaceType:units = "1" ;
SurfaceType:long_name = "Surface Type" ;
SurfaceType:coordinates = "/GEODATA/longitude /GEODATA/latitude" ;
SurfaceType:flag_meanings = "evergreen_needle_forest evergreen_broad_forest deciduous_needle_forest deciduous_broad_forest mixed_forest closed_shrubs open_shrubs woody_savannas savannas grassland wetlands crops urban crop_or_mosaic snow_or_ice barren_or_desert water tundra" ;
SurfaceType:_FillValue = 65535US ;
SurfaceType:valid_min = 0US ;
SurfaceType:valid_max = 65534US ;
SurfaceType:flag_values = 1US, 2US, 3US, 4US, 5US, 6US, 7US, 8US, 9US, 10US, 11US, 12US, 13US, 14US, 15US, 16US, 17US, 18US ;
float VIIRS_confidently_clear(scanline, ground_pixel) ;
VIIRS_confidently_clear:units = "1" ;
VIIRS_confidently_clear:long_name = "VIIRS_confidently_clear" ;
VIIRS_confidently_clear:coordinates = "/GEODATA/longitude /GEODATA/latitude" ;
VIIRS_confidently_clear:_FillValue = -999.f ;
VIIRS_confidently_clear:valid_min = 0.f ;
VIIRS_confidently_clear:valid_max = 1.f ;
float VIIRS_confidently_cloudy(scanline, ground_pixel) ;
VIIRS_confidently_cloudy:units = "1" ;
VIIRS_confidently_cloudy:long_name = "VIIRS_confidently_cloudy" ;

```
            VIIRS_confidently_cloudy:coordinates = "/GEODATA/longitude
/GEODATA/latitude" ;
            VIIRS_confidently_cloudy:_FillValue = -999.f ;
            VIIRS_confidently_cloudy:valid_min = 0.f ;
            VIIRS_confidently_cloudy:valid_max = 1.f ;
      float VIIRS_probably_clear(scanline, ground_pixel) ;
            VIIRS_probably_clear:units = "1" ;
            VIIRS_probably_clear:long_name = "VIIRS_probably_clear" ;
            VIIRS_probably_clear:coordinates = "/GEODATA/longitude
/GEODATA/latitude" ;
            VIIRS_probably_clear:_FillValue = -999.f ;
            VIIRS_probably_clear:valid_min = 0.f ;
            VIIRS_probably_clear:valid_max = 1.f ;
      float VIIRS_probably_cloudy(scanline, ground_pixel) ;
            VIIRS_probably_cloudy:units = "1" ;
            VIIRS_probably_cloudy:long_name = "VIIRS_probably_cloudy" ;
            VIIRS_probably_cloudy:coordinates = "/GEODATA/longitude
/GEODATA/latitude" ;
            VIIRS_probably_cloudy:_FillValue = -999.f ;
            VIIRS_probably_cloudy:valid_min = 0.f ;
            VIIRS_probably_cloudy:valid_max = 1.f ;
 data:
 } // group SCIDATA
}
```